

**pp INTERACTIONS AT 303 GeV/c:
MULTIPLICITY AND TOTAL CROSS SECTION**

**F. T. Dao, D. Gordon, J. Lach, E. Malamud
National Accelerator Laboratory
Batavia, Illinois 60510**

and

**T. Meyer, R. Poster, and W. Slater
University of California, Los Angeles
Los Angeles, California 90024**

October 23, 1972



pp INTERACTIONS AT 303 GeV/c:
MULTIPLICITY AND TOTAL CROSS SECTION

F. T. Dao, D. Gordon, J. Lach, E. Malamud
National Accelerator Laboratory
Batavia, Illinois 60510

and

T. Meyer, R. Poster, and W. Slater*
University of California, Los Angeles
Los Angeles, California 90024

October 23, 1972

ABSTRACT

In an exposure of the 30-in. hydrogen bubble chamber to a 303 GeV/c proton beam, 2245 interactions have been observed. The measured total cross section is 39.0 ± 1.0 mb and the average charged particle multiplicity, $\langle n_{ch} \rangle = 8.86 \pm 0.16$.

*Work supported by the United States National Science Foundation under grant #GP-33565.

EXPERIMENTAL CONDITIONS

In this paper we present data on the interactions of 303 GeV/c protons in the 30-in. hydrogen bubble chamber at the National Accelerator Laboratory. The primary proton beam was extracted from the accelerator and the bubble-chamber beam line was tuned using these protons. The intensity of the beam was then suitably attenuated by closing collimators, defocusing magnets and inserting an aluminum target approximately 1 km upstream of the bubble chamber which was viewed at 1.5 mrad. Measurements indicated that the beam momentum spread was less than 0.5%. The primary proton beam entered the bubble chamber with a very small angular spread, and we believe that within this angular region the fraction of contaminating particles is small.¹

For this run we used the following bubble-chamber parameters: B = 27 kG, 35-mm film, 4 views, bubble size on film ~ 15 μ , and a bubble density for minimum ionizing particles 10-12/cm. The entrance window is ~ 18-cm high by ~ 5.5-cm wide.

EXPERIMENTAL PROCEDURES

All the film was scanned twice, once by a physicist and once by a professional scanner. The chamber was imaged at 90% of its true size. In the first scan a decision was made as to whether a picture was acceptable based on two criteria:

1. All hadron tracks entering the chamber had to be parallel to the beam to $\lesssim 1$ mrad.

2. The number of beam tracks entering through the window as projected in view 2 had to be ≤ 15 .

Frames were also rejected due to chamber malfunction. With these criteria 6201 frames were accepted out of ~16,000 frames taken. The scanners were instructed to record the number of entering beam tracks, all events, any secondary interactions, neutron stars, V's, kinks, Dalitz pairs, and stopping protons as well as any unusual features in the picture. The average number of tracks/accepted frame was 4.9. The beam intensity was adjusted to optimize the product of acceptable pictures and tracks.

The rescan consisted of only the 6201 accepted frames. In a third, or conflict scan, every event was carefully reexamined by one or two physicists, if necessary using magnification a factor of $\sim 9\times$ chamber size.

Scanning was done with no fiducial cut and 2750 events were found. A fiducial volume cut reduced this to our final sample of 2245 events. From the first two scans the scanning efficiency (assuming all events equally easy to find) was computed to be $99.2 \pm 0.2\%$ for two-pronged events; for other topologies it was even higher. For the 1674 events with the number of charged secondaries (n_{ch}) ≥ 4 found in both scans, and assuming the conflict scan topological decision to be correct, 78.2% of the events were correctly identified in both scans, 16.6% of the events were wrongly identified in one scan and 5.2% were wrongly identified in both scans.

The following corrections were applied to the data:

1. Low-t two-prongs. The recoil proton has been measured for all two-prong events with a stopping proton and their t - distribution is plotted in Fig. 1. The detection efficiency is $> 99\%$ for the t range $0.02 \leq (-t) \leq 0.12 \text{ (GeV/c)}^2$. For smaller t the scanning efficiency drops.

The extrapolation to $t = 0$ using the functional form $d\sigma/dt \propto ke^{bt}$ yields 52 ± 8 undetectable or undetected two-prongs in the experiment.

2. Disposition of odd-prong events, close secondary interactions and low-t recoils. There are 25 odd-prong events. These may be due to an undetectable low- t proton or an unresolvable secondary interaction close to the primary vertex. The latter mostly affect high-multiplicity events. There are 528 secondary interactions produced from events in the fiducial volume. A plot of their distance from the primary vertex reveals that ~ 16 secondary interactions were possibly missed within 2.2 cm of the primary. All stopping proton events in the film have been measured. A study of the Chew-Low plot for $n_{\text{ch}} \geq 4$ shows a depletion of ~ 12 events for $|t| \leq 0.02 \text{ (GeV/c)}^2$. If the odd-prong events are due to close secondaries they should be shifted to a lower multiplicity bin. If they are due to unseen low- t recoils they should be shifted to the next higher multiplicity bin. In preparing the table of topological cross sections these odd-prong events have been split evenly between adjacent even topology bins; the effect on the moments of the multiplicity distribution of shifting them all up or all down is discussed below.

3. Close V's. There are 514 V's produced by interactions in the fiducial volume. Of these ~100 are obvious electron pairs. A plot of the distance between the primary vertex and secondary vertex shows that ~25 V's were missed within 2.2 cm of the primary vertex. Correcting for these V's would lower the multiplicity. This correction is small compared to the present level of statistical accuracy so is not applied to the topological cross sections. However, its effect on the moments is shown below.

4. Dalitz pairs. It is assumed that the average number of π^0 's is one half the average number of charged π 's, that the average number of K^\pm is 10% of the π^\pm , and that the average number of protons is 1.4. Thus, $\langle n_{\pi^0} \rangle \approx 3.4$ and 2245 events will contain ~88 Dalitz pairs. The 24 observed Dalitz pairs have been used to make the correction to the topological cross sections. The corrected number, 88, is distributed among topologies in the same way as the observed 24.

RESULTS

Total Cross Section

The total cross section measured in this experiment is 39.0 ± 1.0 mb based on 2245 observed events. Besides the statistical error we have included a 1% uncertainty in the density of liquid hydrogen used, 0.0625 g/cm³, and a 1% uncertainty in the average potential path of 53.05 cm. The contribution to the uncertainty arising from the correction for events lost at low-t is negligible.

The slope parameters determined by Barbiellini et al.² and our measured total cross section give elastic-scattering cross section of 7.2 ± 0.4 mb computed using the optical theorem. A plot of measured total cross sections as a function of laboratory momenta is shown in Fig. 2. All measurements from 30 GeV/c to 500 GeV/c are consistent with a constant pp cross section of 38.5 mb.

Table I. Topological Cross Sections at 303 GeV/c.

n_{ch}	Events Found	Corrected Number ^a	Cross Section ^b
1		529 ± 23	7.2 ± 0.4 mb
2	475	$\left. \begin{array}{l} \text{el. } 424 \pm 24 \\ \text{inel. } 105 \pm 33 \end{array} \right\}$	
3	1		
4	278	285 ± 17	4.84 ± 0.30
5	2		
6	329	336 ± 19	5.71 ± 0.34
7	6		
8	311	318 ± 19	5.40 ± 0.33
9	5		
10	274	278 ± 18	4.72 ± 0.32
11	2		
12	245	247 ± 17	4.19 ± 0.30
13	2		
14	127	128 ± 12	2.17 ± 0.21
15	4		
16	83	82 ± 10	1.39 ± 0.17
17	1		
18	52	51 ± 8	0.87 ± 0.14
19	1		
20	31	30 ± 6	0.51 ± 0.11
21	0		
22	5	4 ± 3	0.07 ± 0.06
23	1		
24	6	6 ± 3	0.10 ± 0.05
25	0		
26	4	3 ± 2	0.05 ± 0.03
Total	2245	2297	39.0 ± 1.0

^aCorrected for low- t two-prongs and Dalitz pairs; odd-prong events distributed as discussed in text.

^bThese errors contain an additional uncertainty contributed by hydrogen density and track-length errors.

The multiplicity distribution is shown in Fig. 3 together with a Poisson distribution normalized to $\langle n_{ch}^- \rangle$, the average number of negative secondaries. This curve is a poor fit to the data. In Fig. 4 the scale is expanded to show the high multiplicity cross sections in more detail and compared with a $1/n_{ch}^2$ functional form which is also a poor representation of the data.

The moments of the multiplicity distribution are shown in Table II.

Table II. Moments of the Multiplicity Distribution.

	All Prongs	Negative Only
$\langle n \rangle$	8.86 \pm 0.16	3.428 \pm 0.079
$\langle n^2 \rangle$	97.6 \pm 2.9	16.55 \pm 0.57
$\langle n^3 \rangle$	(1.261 \pm 0.054) $\cdot 10^3$	96.7 \pm 4.9
$\langle n^4 \rangle$	(1.84 \pm 0.11) $\cdot 10^4$	649 \pm 46
$\langle n^5 \rangle$	(2.96 \pm 0.24) $\cdot 10^5$	(4.84 \pm 0.47) $\cdot 10^3$
$\langle n \rangle (\langle n^2 \rangle - \langle n \rangle^2)^{-\frac{1}{2}}$	2.022 \pm 0.062	1.568 \pm 0.054
g_2^a	88.8 \pm 2.7	13.12 \pm 0.50
g_3	987 \pm 46	54.0 \pm 3.4
g_4^a	(1.186 \pm 0.081) $\cdot 10^4$	230 \pm 23
f_2^b	10.31 \pm 0.92	1.36 \pm 0.25
f_3	17.1 \pm 6.1	-0.40 \pm 0.74
f_4	-88 \pm 48	-4.59 \pm 2.25

^{a, b} See Ref. 5. Note: $n = n_{ch}$

In Table III we examine the sensitivity of $\langle n \rangle$ and $\langle n(n-1) \rangle$ to the various experimental details.

Table III. Sensitivity of Moments to Experimental Details.

Final experimental value	8.86 ± 0.16	88.8 ± 2.7
	Change in $\langle n_{ch} \rangle$ In Standard Deviations	Change in $\langle n_{ch}(n_{ch} - 1) \rangle$ In Standard Deviations
No fiducial cut (2750 events)	-0.9	-1.1
First scan only (no fiducial cut)	-0.9	-1.4
Second scan only (no fiducial cut)	-0.6	-1.0
Omitting low-t, two-prongs	0.9	0.7
Using $\sigma_{el} = 6.8$ mb instead of 7.2 mb	-0.6	-0.4
Omitting Dalitz pair correction	0.5	0.7
Putting in a close V correction	-0.2	-0.1
Shifting odd-prong events to lower multiplicity bins	-0.2	-0.1
Shifting odd-prong events to higher multiplicity bins	0.2	0.1

CONCLUSIONS

It is interesting to study the s- dependencies of the various quantities in this experiment.

In Figs. 5(a) and (b) are plotted the topological cross section. At 303 GeV/c the two, four, and six prong are decreasing with no sign of leveling off, the eight and ten prongs are roughly constant, and all the cross sections for $n_{ch} \geq 12$ are increasing.

$\langle n_{\text{ch}} \rangle$ is shown in Fig. 6. The four bubble-chamber experiments spanning 50 - 300 GeV/c do not appear to follow a simple $\ln p_{\text{lab}} (\sim \ln s)$ dependence; $\langle n_{\text{ch}}(n_{\text{ch}} - 1) \rangle$ is shown in Fig. 7. Berger⁴ fits the momentum dependence of this quantity for two general models and extrapolates the fit to our momentum. His extrapolated prediction yields a value of 77 for a multiperipheral model and 84 for a fragmentation model. Our value of 89 ± 3 is in closer agreement with the latter.

Finally, in Fig. 8 $\langle n_{\text{ch}} \rangle (\langle n_{\text{ch}}^2 \rangle - \langle n_{\text{ch}} \rangle^2)^{-\frac{1}{2}}$ is shown. The apparent constancy of this expression has been noted by a number of authors⁵ and in particular Koba, Nielsen, and Olesen point out it follows from one of their scaling laws.

ACKNOWLEDGMENTS

Significant scientific contributions to this work have been made by many physicists other than the authors. They have built and operated the NAL accelerator, its extraction system, and the hadron beam line to the bubble chamber. It has been a privilege for us to work with them during the course of this experiment, and we thank them for their enthusiastic participation. We gratefully acknowledge the dedicated support of the operations staffs of the accelerator, the Neutrino Laboratory, the 30-in. Bubble Chamber, and Film Analysis Facility.

REFERENCES

¹One can show that the π^+ contamination in our beam was negligible by the following argument. If one looks at the relative rates of π^+ to proton production as predicted by Hagedorn and Ranft at a secondary momentum 5% less than the incident momentum, one finds the ratio $\pi^+/p \leq 10^{-6}$. Since our beam-momentum bite was measured to be less than 0.5% we feel the π^+ contamination to be totally negligible. By demanding a tight-angle tolerance on tracks entering the bubble chamber we also feel the muon contamination to be negligible.

²G. Barbiellini et al. Phys. Letters 39B, 663 (1972). Interpolation of the b parameters measured in this experiment at $s = 462 \text{ GeV}^2$ and 949 GeV^2 is used to obtain b parameters at $p_{\text{lab}} = 300 \text{ GeV}/c$.

³Definitions of f_n and g_n

$$g_1 = \langle n \rangle$$

$$g_2 = \langle n(n-1) \rangle$$

$$g_3 = \langle n(n-1)(n-2) \rangle$$

$$g_4 = \langle n(n-1)(n-2)(n-3) \rangle$$

$$f_2 = g_2 - g_1^2$$

$$f_3 = g_3 - 3g_2g_1 + 2g_1^3$$

$$f_4 = g_4 - 4g_1g_3 + 12g_1^2g_2 - 3g_2^2 - 6g_1^4$$

⁴E. L. Berger, Phys. Rev. Letters 29, 887 (1972).

- ⁵O. Czyzewski and K. Rybicki, Crowkov report INP No. 800/PH (1972);
Z. Koba, H. B. Nielsen, and P. Olesen, Nucl. Phys. B40, 317 (1972);
S. N. Ganguli and P. K. Malhotra, Tata Institute preprint TIFR-BC-72-6,
July 1972.
- ⁶S. P. Denisov et al., Phys. Letters 36B, 415 (1971).
- ⁷V. Bartenev et al., Small Angle Elastic Proton-Proton Scattering
from 25 to 200 GeV, submitted to the XVI International Conference on
High Energy Physics, September 1972.
- ⁸J. W. Chapman et al., A Measurement of the Charged-Particle
Multiplicity in pp Collisions at 102 GeV/c, Rochester-Michigan
Collaboration, University of Rochester Report #UR-395, submitted
to the XVI International Conference on High Energy Physics,
September 1972.
- ⁹G. Charlton et al., Phys. Rev. Letters 29, 515 (1972).
- ¹⁰M. Holder et al., Phys. Letters 35B, 361 (1971).
- ¹¹G. Alexander et al., Phys. Rev. 154, 1284 (1967).
- ¹²D. B. Smith et al., Phys. Rev. Letters 23, 1064 (1969) and University
of California Radiation Laboratory Report UCRL-20632, March 1971.
- ¹³H. Boggild et al., Nucl. Phys. 27B, 285 (1971).
- ¹⁴Soviet-French Mirabelle Collaboration, submitted to the XVI Inter-
national Conference on High Energy Physics, September 1972.
- ¹⁵M. Breidenbach et al., Phys. Letters 39B, 654 (1972).

FIGURE CAPTIONS

- Fig. 1. t distribution for events having a stopping proton.
- Fig. 2. A compilation of pp total cross sections as a function of laboratory momentum.
- Fig. 3. Cross section for individual multiplicities.
- Fig. 4. Expansion of cross-section data for high multiplicities.
- Fig. 5(a)(b). Summary of energy dependence of topological cross sections as a function of p_{lab} .
- Fig. 6. $\langle n_{ch} \rangle$ as a function of p_{lab} .
- Fig. 7. $\langle n_{ch} (n_{ch} - 1) \rangle$ as a function of p_{lab} .
- Fig. 8. $\langle n_{ch} \rangle (\langle n_{ch}^2 \rangle - \langle n_{ch} \rangle^2)^{-\frac{1}{2}}$ as a function of p_{lab} .

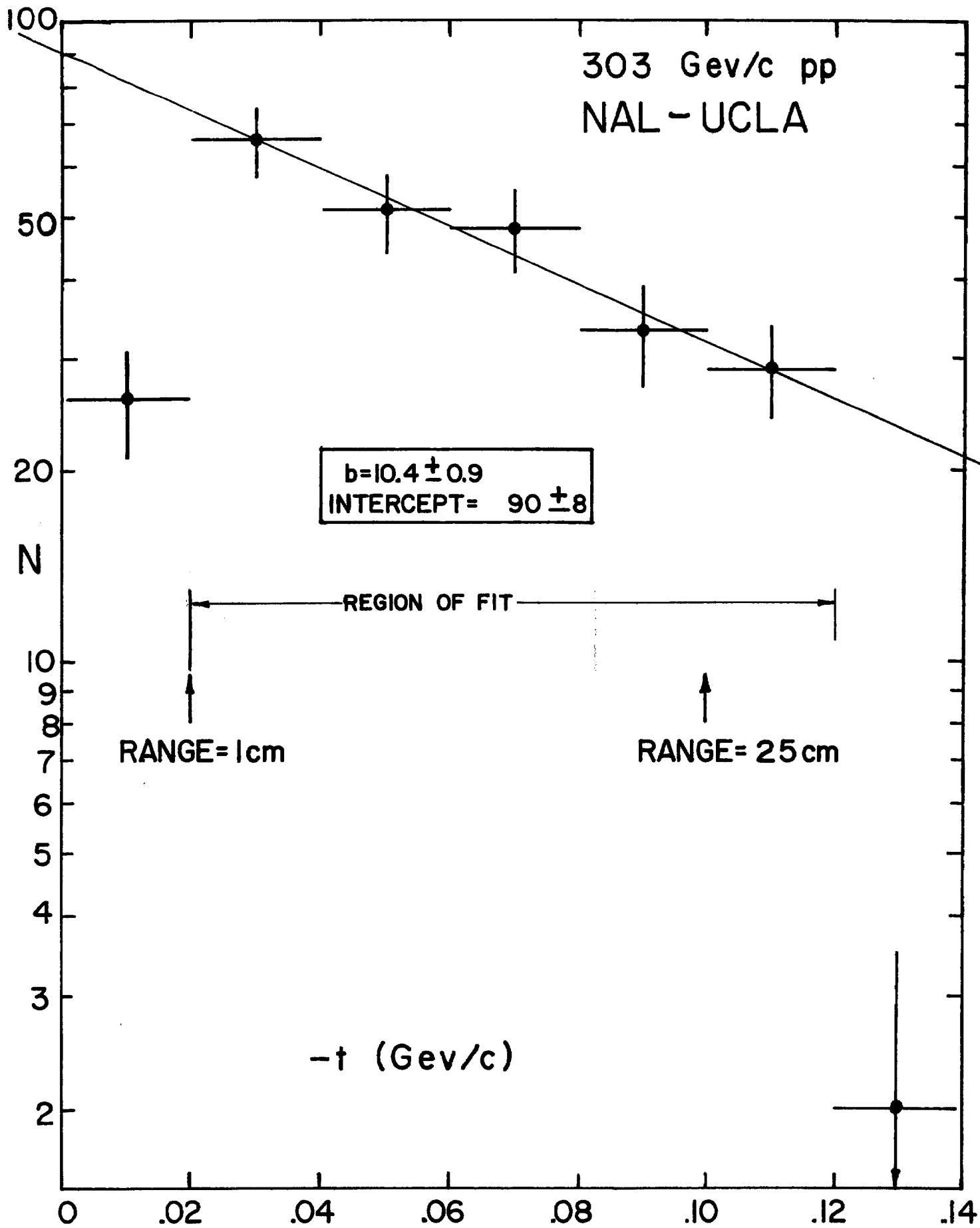


Figure 2

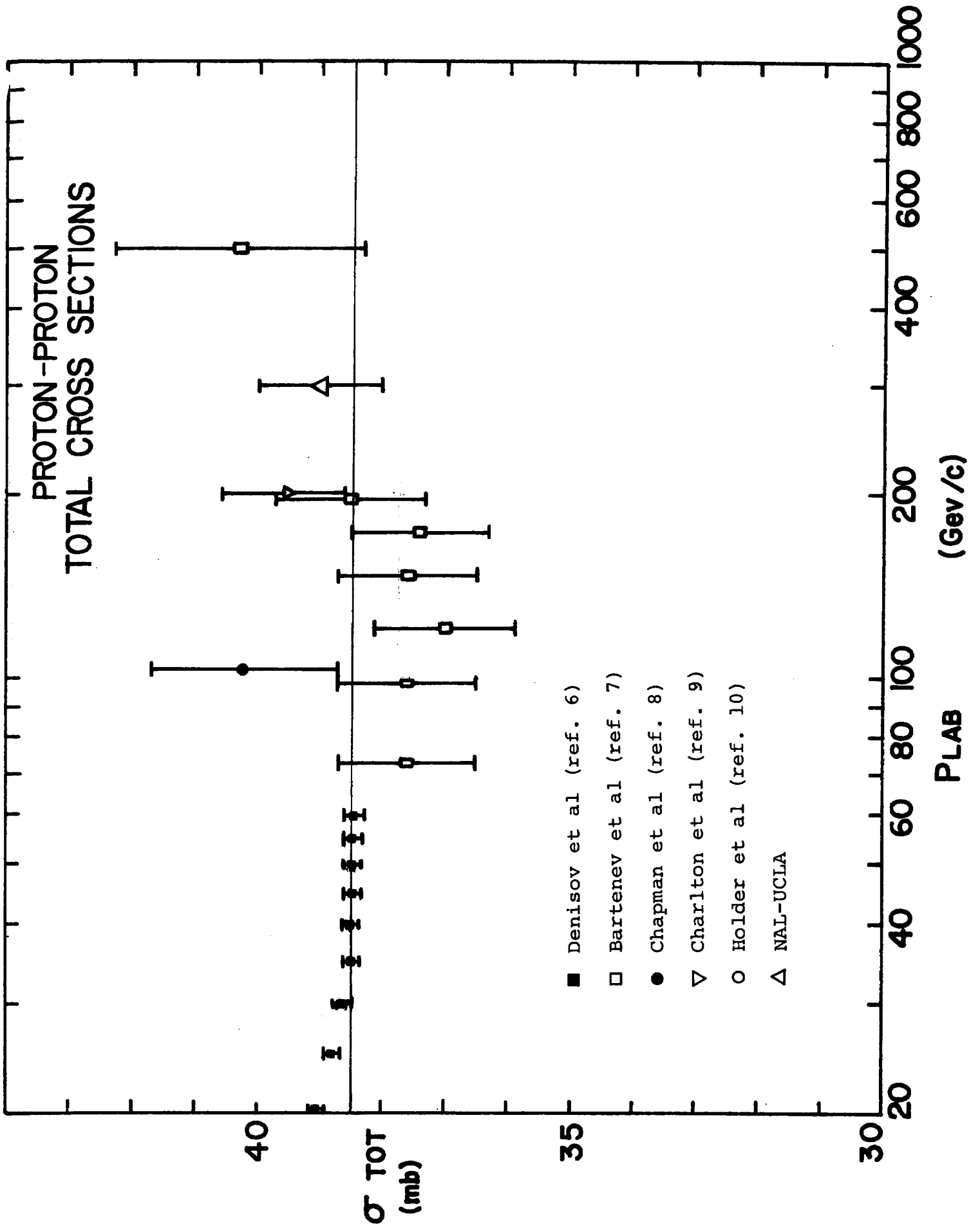
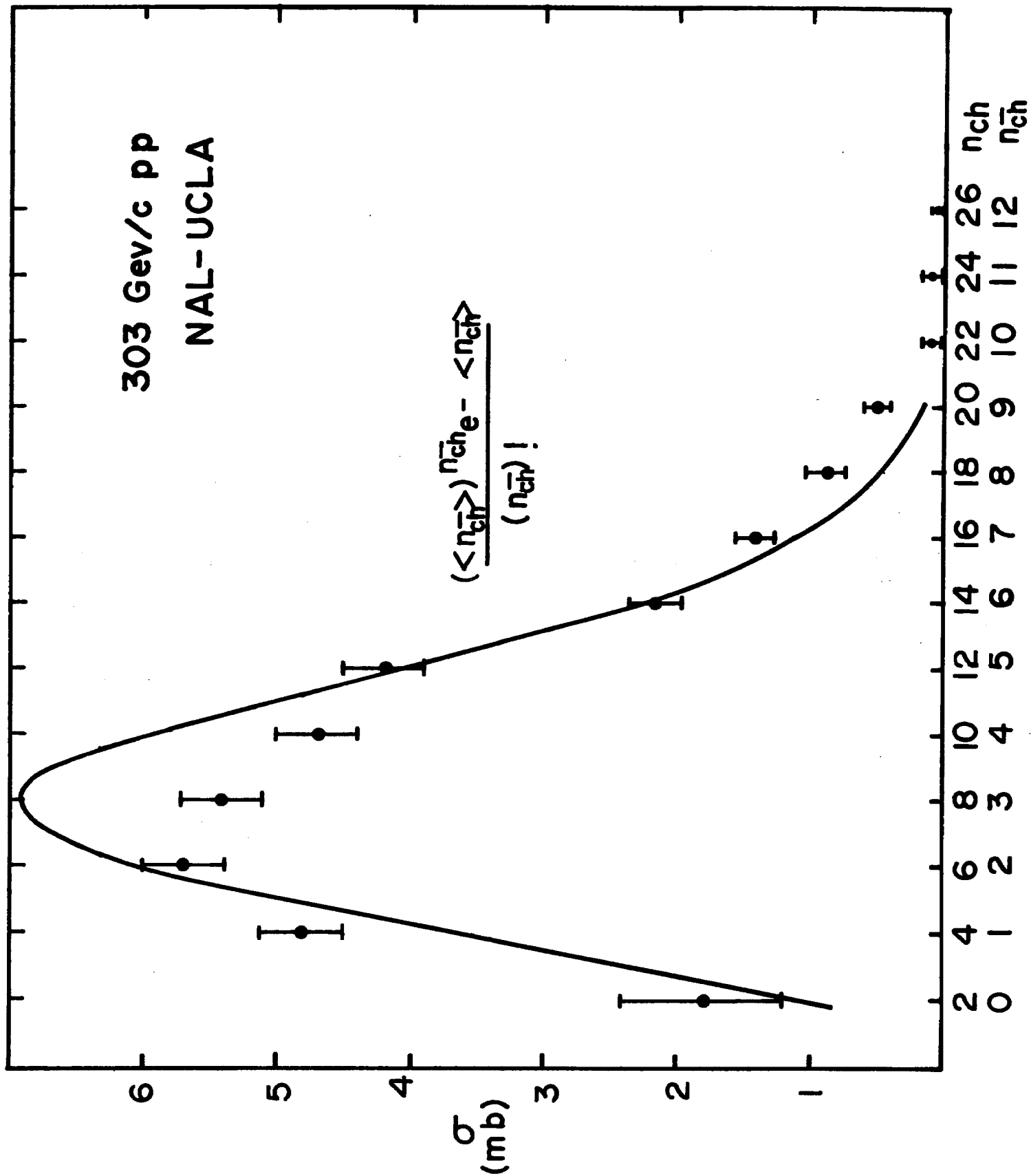


Figure 3



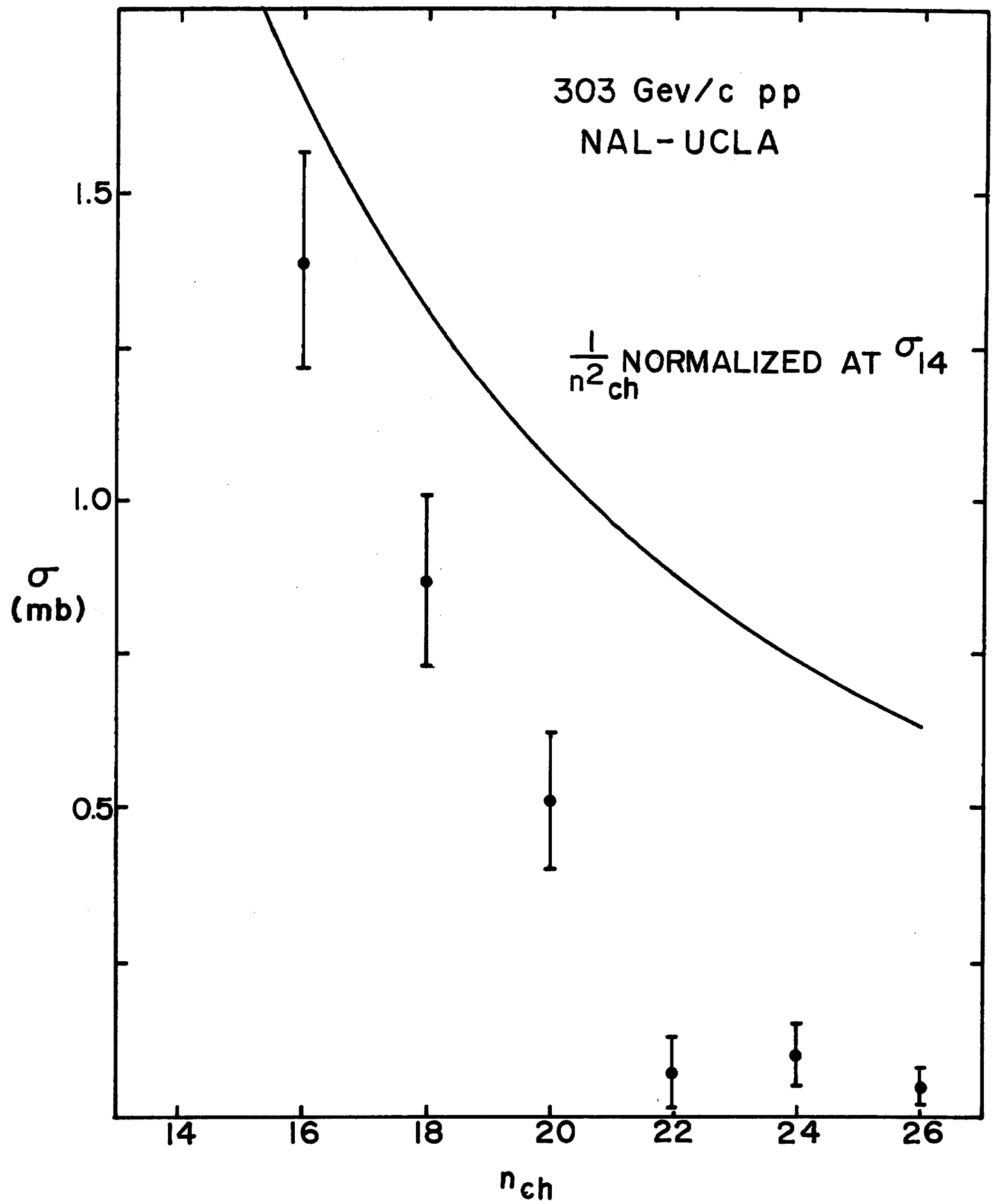


Figure 5a

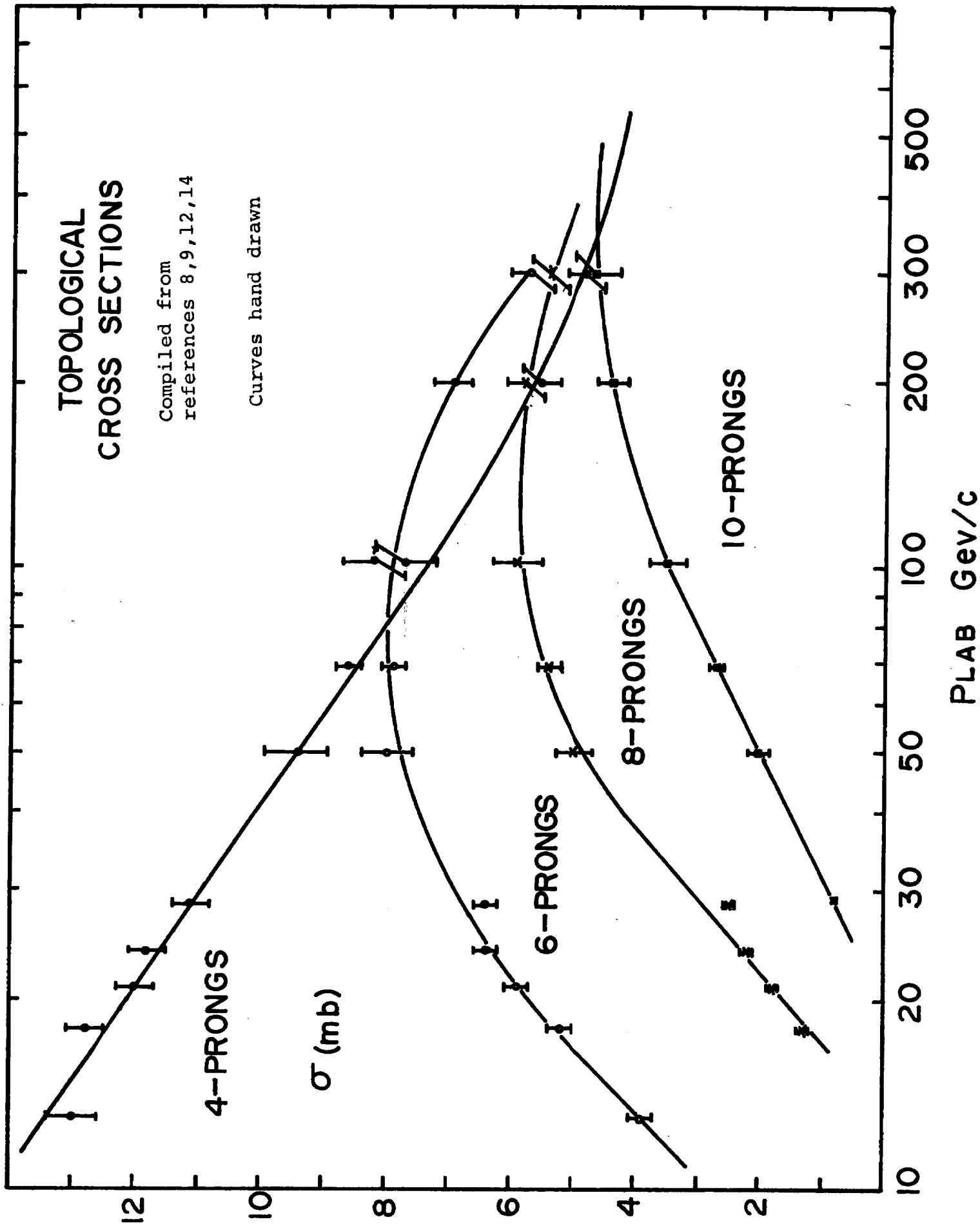


Figure 5b

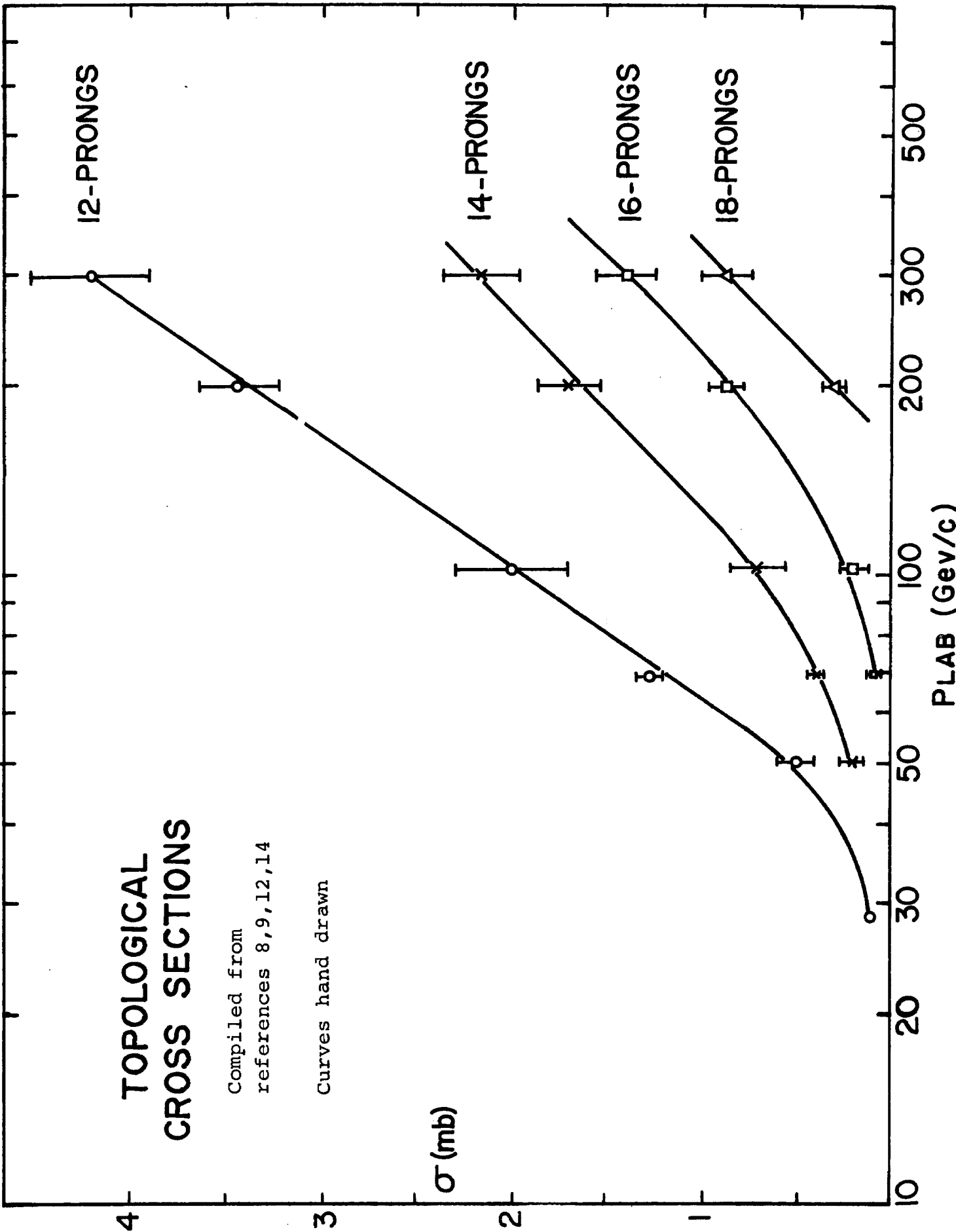


Figure 6

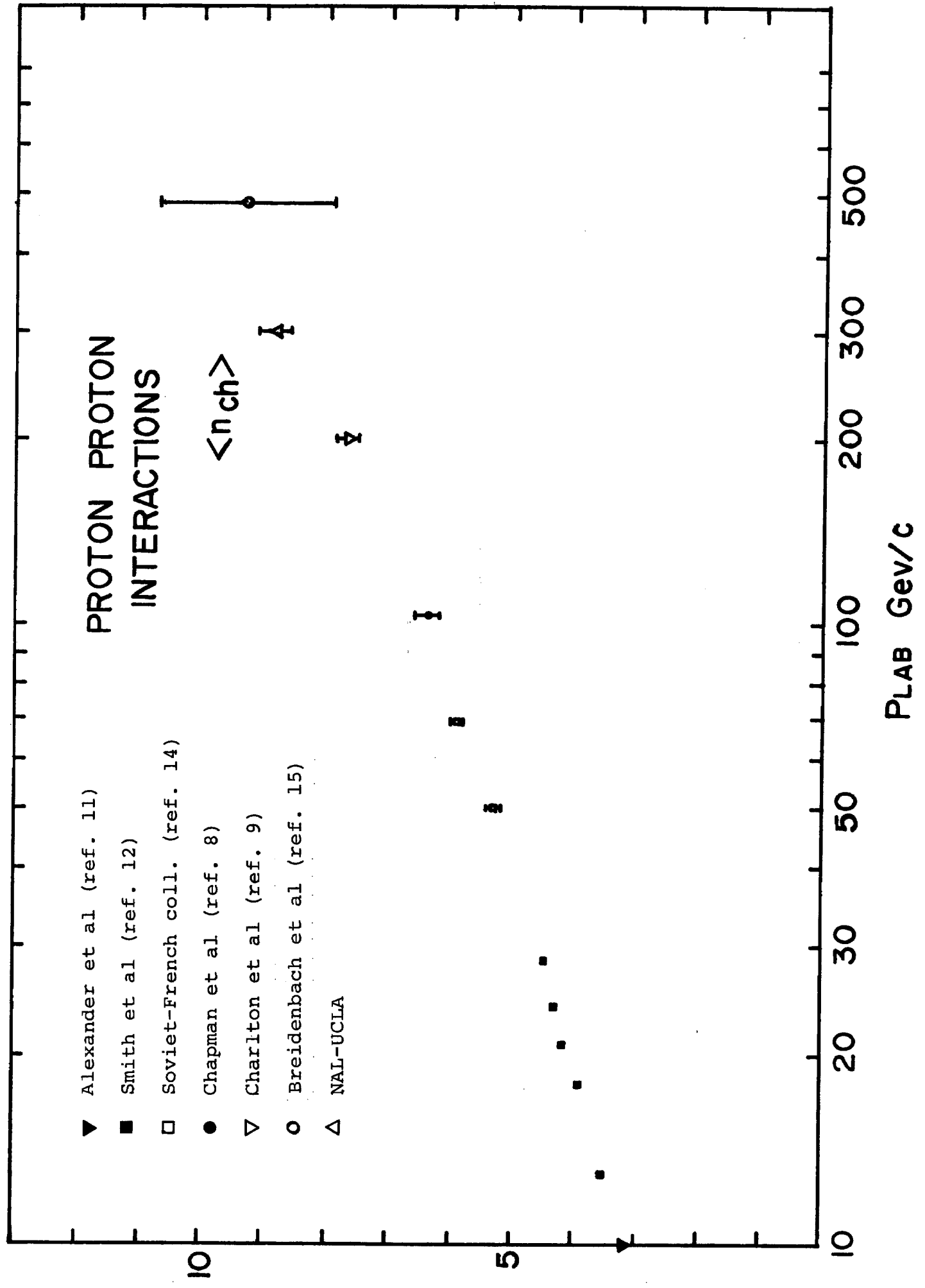


Figure 7

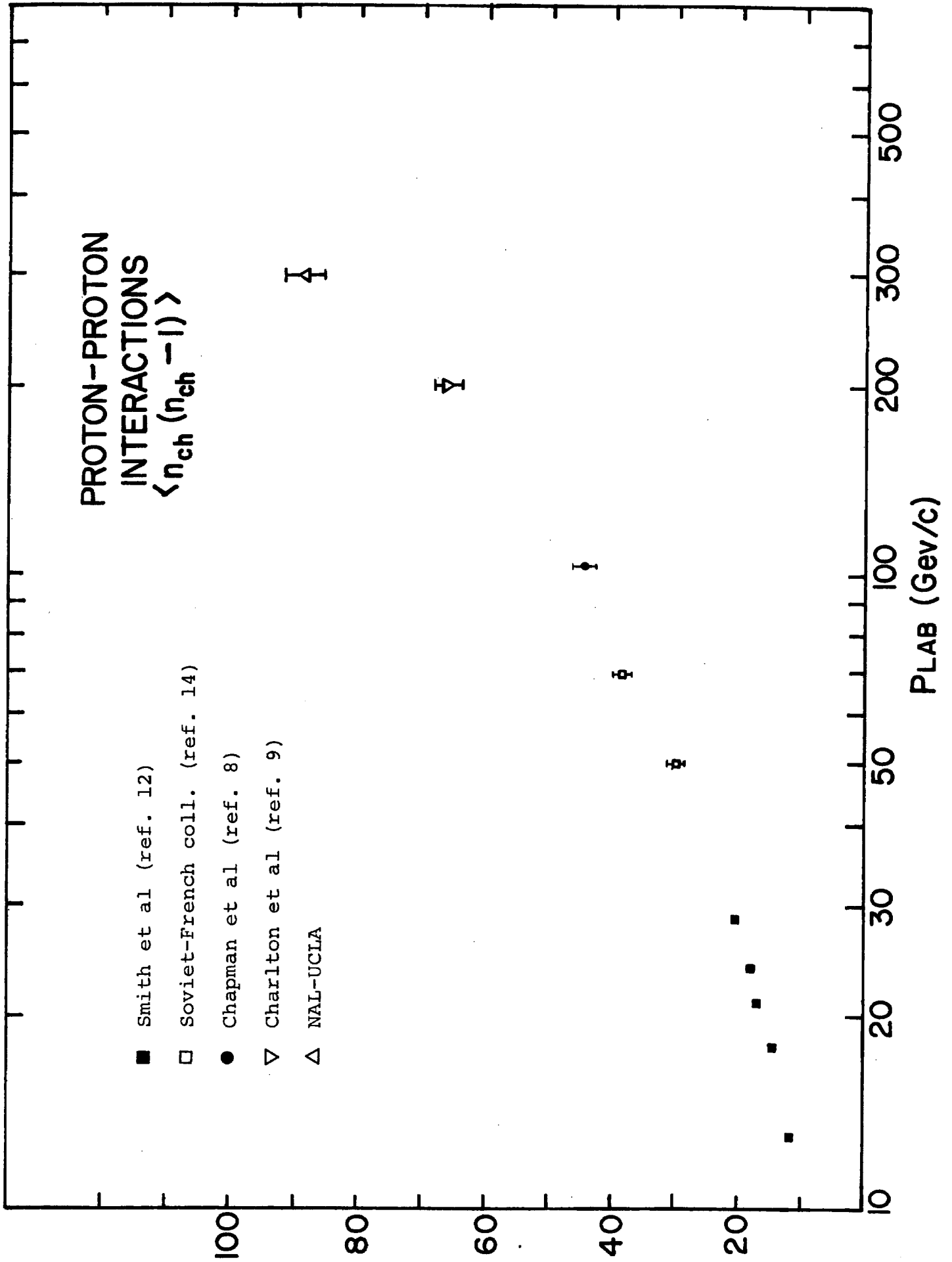


Figure 8

